Quantitative Comparison of Partitioned-Stator Machines for Hybrid Electric Vehicles

Christopher. H. T. Lee, *Member, IEEE*, James L. Kirtley, Jr., *Life Fellow, IEEE*, M. Angle, *Member, IEEE*, and Heng Nian, *Senior Member, IEEE*

***Abstract*—In this paper, three partitioned-stator (PS) machines, namely the PS flux-switching DC-field (PS-FSDC) machine, the PS-FS hybrid-excitation (PS-FSHE) machine, and the flux adjuster FS permanent-magnet (FA-FSPM) machine are proposed. With different flux-regulating mechanisms, all three proposed machines can offer satisfactory flux-weakening capabilities for wide-speed range operations. Unlike the traditional PS machine that installs the armature windings and the excitation sources in the outer-stator and inner-stator, respectively; the proposed machines purposely swap the installation arrangements. Upon the proposed structure, the FA-FSPM machine can fully utilize the stator core for PM material accommodations. As a result, excellent power and torque densities can be achieved. To verify the proposed concepts, these three PS machines are quantitatively compared based on the hybrid electric vehicle (HEV) specifications.**

***Index Terms*—Flux-weakening, hybrid electric vehicle, hybrid-excitation, mechanical flux adjuster, partitioned-stator.**

I. Introduction

SINCE the energy crisis and environmental pollution have become the growing problems recently, as one of the most promising solutions, the development of the hybrid electric vehicles (HEVs) has drawn many attentions [1-3]. As the key component of HEVs, the electric machines have to fulfill some distinguished requirements as [4-6]:

- high efficiency,
- high power and torque densities,
- high controllability,
- wide-speed range,
- maintenance-free operation, and
- high cost-effectiveness.

The flux-switching permanent-magnet (FSPM) machine is able to accomplish most of these tasks and this type of machine has been developed rapidly in the past few decades [7-9]. To further improve its power and torque densities, the partitioned-stator FSPM (PS-FSPM) machine, which utilizes the inner space to accommodate the armature winding, has been proposed [10]. However, inheriting the characteristics of the PM machines, the FSPM and PS-FSPM candidates both suffer from the low flux-regulating capabilities.

To improve the flux-weakening capabilities for wide-speed range operations, the advanced magnetless machines have become a hot research topic recently [11, 12]. In principle, the magnetless machine employs the DC-field windings as the excitation fields, and hence it can control its flux density very effectively. Nevertheless, without the installation of the high-energy-density PM materials, the magnetless machines generally suffer from lower power and torque densities than the PM counterparts do. To overcome the demerits of the magnetless machines, the concept of hybrid-excitation (HE) topology has been developed actively [13-15]. Upon the implementation with two excitation sources, namely the DC-field windings and PM materials, the HE machines can take the benefits from both sides. Yet, the DC-field excitations produce undesirable copper losses and the benefits from flux-weakening operation are partially offset.

The mechanical flux adjusters (FAs), which short-circuit the PM fluxes to achieve flux-weakening operation, has been proposed [16]. With the installation of FAs, the PM machines not only can enjoy the benefits from its ancestors do, but also achieve excellent flux-weakening capabilities without extra copper losses. However, the discussions on the FA machine still focus on the conventional machine topology, while the researches on the PS structure are still very limited [17].

The purpose of this paper is to implement the FA structure into the PS-FSPM machine, hence producing the proposed FA-PS-FSPM machine. The proposed PS machine purposely installs the PM materials in the outer-stator. As a result, with the proposed structure, the mechanical FAs no longer shares the space with the PM materials anymore. To verify the proposed machine designs, the PS-FSDC machine and the PS-FSHE machine will be included for comparisons based on the requirements for HEV applications.

II. Hybrid Electric Vehicle Architecture

The typical HEV structure, which installs the electric machines as the major power device for normal operations and the internal combustion engine (ICE) as the supplementary device for range extension, is shown in Fig. 1. With the support of the electric machine, the HEV can offer the regenerative braking operation, so that the battery can be recharged when the HEV undergoes braking conditions. Hence, the overall fuel efficiency of the HEV systems can be greatly improved.

This work was supported by Croucher Foundation, Hong Kong Special Administrative Region, China and Jiangsu Xinri E-Vehicle Co., Ltd., Wuxi, Jiangsu, China.

C. H. T. Lee, J. L. Kirtley, and M. Angle are with the Research Laboratory of Electronics, Massachusetts Institute of Technology, Cambridge, MA, USA (e-mail: chtlee@mit.edu; kirtley@mit.edu; mangle@mit.edu).

James L. Kirtley Jr. is a Professor of Electrical Engineering at the Massachusetts Institute of Technology (MIT).

H. Nian is with the College of Electrical Engineering, Zhejiang University, Hangzhou 310027, China (e-mail: nianheng@zju.edu.cn).

As the key component of the HEVs, the electric machines have to fulfill various criteria as listed in [7]. Even though the targeted specifications may vary among different applications, the HEV in general has to offer three major operations, namely the engine cranking, the torque boosting and the flux-weakening operations.

A. Operation I: Engine Cranking

When the HEV is idle for a long period of time, the electric machine should produce a starting torque to start up the engine. This sequential action is so-called as the cold cranking. The advanced HEV purposely turns off the engine during the cruising operation such that the overall fuel economy can be improved. As a result, the electric machine needs to provide cranking frequently, and it is so-called as the warm cranking. The electric machine needs to produce satisfactory torque levels for the two cranking operations.

B. Operation II: Torque Boosting

When the HEV has to speed up or climb uphill, the electric machine should boost up the torque level to the peak value for a short period of time, say for a couple of seconds. At this moment, the electric machine has to strengthen its flux densities to produce the maximum torque. As a result, the output torque can be increased to satisfy the driver's needs. This is sometimes known as the flux-strengthening or torque boosting operations.

C. Operation III: Flux-Weakening

When the HEV is sped up after the torque boosting mode, the regenerated electromotive forces (EMFs) among the armature windings also increase in accordance to the operating speeds. The electric machine should weaken the flux densities in order to maintain the constant power level within the high speed region. As a result, high machine efficiency can be maintained in a wide operating range. This operating mechanism is so-called as the flux-weakening mode.

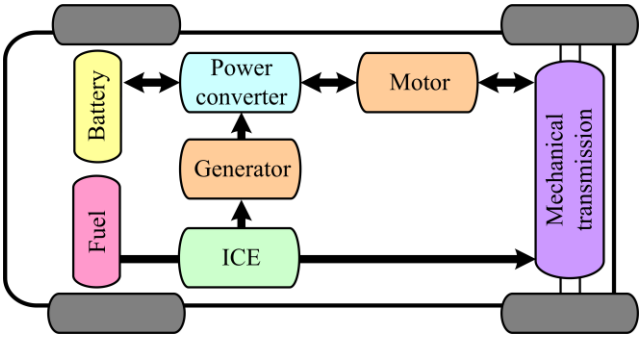

Fig. 1. Typical hybrid electric vehicle structure.

III. PROPOSED PARTITIONED-STATOR MACHINES

A. Machine Structures

The proposed PS-FSDC machine, the PS-FSHE machine and the FA-PS-FSPM machine are shown in Fig. 2. All three proposed machines employ similar topology with the 3-phase 12/10-pole double-stator sandwiched-rotor structure. The conventional PS machine usually installs the armature windings and the excitation sources in the outer-stator and the inner-stator, respectively. On the other hand, the proposed PS machines instead place these two items with the reversed arrangement, i.e., the armature windings are placed in the inner-stator, while the excitation sources in the outer-stator.

Since the three proposed machines are the extension from the profound FSPM machine, their fundamental design equations can be derived from its ancestors [6]. The three proposed machines can be distinguished by their unique excitation sources, i.e., (i) the PS-FSDC machine employs the DC-field windings as the excitation source; (ii) the PS-FSHE machine employs both the DC-field windings and PM materials; and (iii) the FA-PS-FSPM machine employs only the PM materials.

All the proposed machines, namely the PS-FSDC machine, the PS-FSHE machine, and the FA-PS-FSPM machine are designed based on the targeted specifications of the passenger HEV applications [7]. To quantitatively compare these machine in the fair conditions, all the key machine details, namely the outside diameters, stack lengths, and airgap lengths are set equal. In addition, the split ratios, pole arcs, pole heights, winding slot areas and PM volumes are optimized so that the magnetic saturations and core losses can be both reduced.

B. Operating Principles

Since all the three PS machines are developed based on the FSPM machine, these proposed machines all exhibit the bipolar flux-linkage characteristics. To show the bipolar flux-linkage pattern, the flux paths of the FA-PS-FSPM machine are purposely shown in Fig. 3. It can be shown that when the sandwiched-rotor rotates from position 1 to 2, the flux paths interchange its directions accordingly. In order word, the flux polarities and flux-linkages are interchanged. As a result, higher power and torque densities can be produced, as compared with the unipolar counterparts [4].

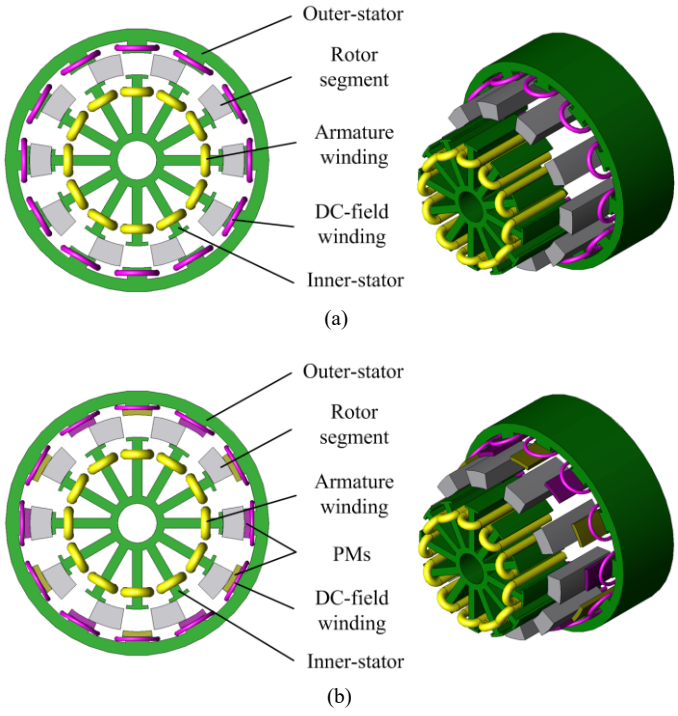

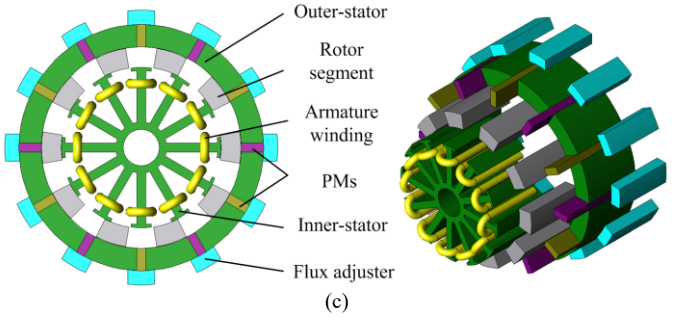

Fig. 2. Proposed machines: (a) PS-FSDC. (b) PS-FSHE. (c) FA-PS-FSPM.

All the three proposed machines exhibit the bipolar flux-linkage characteristics and all of their no-load EMF waveforms should consist of very sinusoidal-like patterns. Hence, the conventional brushless AC (BLAC) conduction scheme should be employed [6]. In particular, the sinusoidal armature current I is injected with respect to the waveform of the bipolar flux-linkage Ψ. As a result, a steady electromagnetic torque T can be produced. The theoretical waveform of this conduction scheme is shown in Fig. 4, while its armature currents can be described as:

$$\begin{cases} i_a = I_{peak} \sin\theta \\ i_b = I_{peak} \sin(\theta - (2\pi/3)) \\ i_c = I_{peak} \sin(\theta + (2\pi/3)) \end{cases} \quad (1)$$

where i_a, i_b, i_c are the armature currents of different phases and I_{peak} is the peak value of the corresponding armature currents.

C. Flux-Regulating Capabilities

As aforementioned, the flux-strengthening and flux-weakening operations, or sometimes known as the flux-regulating capabilities are indispensable for the modern HEV applications. Based on the distinguished machine structures, all the proposed PS machines inherit excellent flux-regulating capabilities to fulfill the HEV requirements.

Upon the installation of the controllable DC-field windings as the only excitation source, the PS-FSDC machine can effectively regulate its flux densities based on the H-bridge converter. Even though the hybrid PS-FSHE machine installs both DC-field windings and PM materials as the excitation sources, it also holds satisfactory flux-regulating capability similar as the PS-FSDC machine does. To be specific, the hybrid machine relies on the PM materials to provide the fundamental excitation field, while it employs the DC-field windings for flux-regulation, as shown in Fig. 5(a). As a result, both the two PS-FSDC and PS-FSHE machines can regulate the flux densities based on the DC-field excitations effectively.

Unlike the PS-FSDC and PS-FSHE machines that employ the external fields for flux-regulations, the proposed FA-FSPM machine instead utilizes the mechanical FAs for flux-weakening operation. With the help of the mechanical device, i.e., an external machine set, the FAs can be inserted to short-circuit the PM fluxes, as shown in Fig. 5(b). In particular, two different arrangements, namely with FAs, and without FAs installations can be achieved. Since the proposed machine installs the PM materials in the outer-stator, the FAs can then be inserted in the outer shell of the outer-stator. As compared with the previous design [17], i.e., the PM materials and the FAs are placed together to share the common space in the inner-stator, the proposed one can fully utilize the whole machine dimension for PM material accommodations.

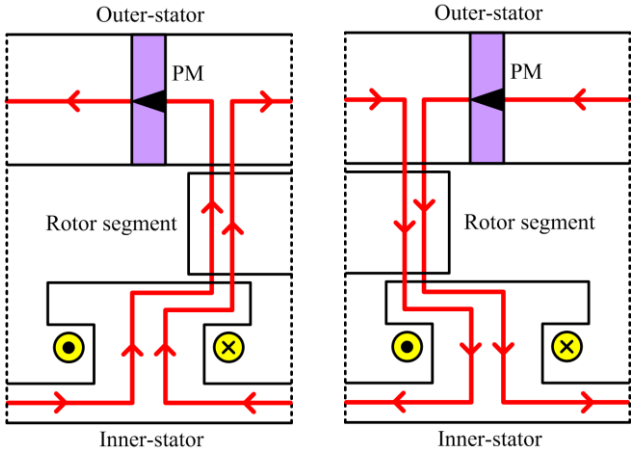

Fig. 3. Flux flow patterns of FA-PS-FSPM: (a) Position 1. (b) Position 2.

IV. Machine Performance Analysis

A. Electromagnetic Field Analysis

As one of the most reliable tools for electric machine analysis, the electromagnetic field analysis is employed in this paper [6]. To be specific, a well-established commercial finite element method (FEM) software, the JMAG-Designer is chosen to analyze the machine performances. Through the iteration mechanisms, the key data of the proposed machines can be optimized. All three proposed machines can then be compared with the quantitative data fairly, while the key design parameters are listed in Table I. It should be noted that the total volume of the FAs are about 470000 mm^3, which is approximately 9.8 % of the machine itself.

The magnetic field distributions of the proposed machines at no-load conditions are shown in Fig. 6. As illustrated, the magnetic field distributions of all three proposed machines are very balanced, while no observable saturations are investigated. As a result, it can be suggested that the proposed machines have been optimized after the iterations so that the minimized power losses should be resulted.

The airgap flux densities of the proposed machines under flux-regulating situations are shown in Fig. 7. As suggested, with the support of the controllable DC-field excitations, the PS-FSDC and PS-FSHE machines can regulate its airgap flux densities effectively, for both flux-strengthening and flux-weakening situations. Meanwhile, upon the utilization of the mechanical FAs, the FA-PS-FSPM machine can also achieve satisfactory flux-weakening capability.

B. Flux-Linkage Analysis

The flux-linkage waveforms of the three proposed machines are shown in Fig. 8. As all three machines show the flux-linkage waveforms with the bipolar characteristics, the design equation as well as the machine structures are confirmed

as correct. Moreover, all the flux-linkage waveforms are in the very balanced shapes with no significant distortions. Therefore, it gives extra evidence to suggest that all the machine structures have been well optimized.

Since the PS-FSDC machine relies barely on the relatively low-energy-density DC-field for field excitation, it results the lowest flux-linkage magnitudes among its counterparts. On the other hand, the FA-PS-FSPM machine enjoys a better space utilization for PM accommodations, such that it can achieve the highest flux-linkage values among the group. As a result, it can be expected the FA-PS-FSPM machine can produce the highest power and torque densities among the three candidates.

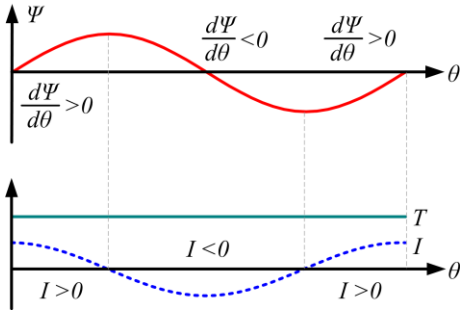

Fig. 4. Theoretical operating waveform.

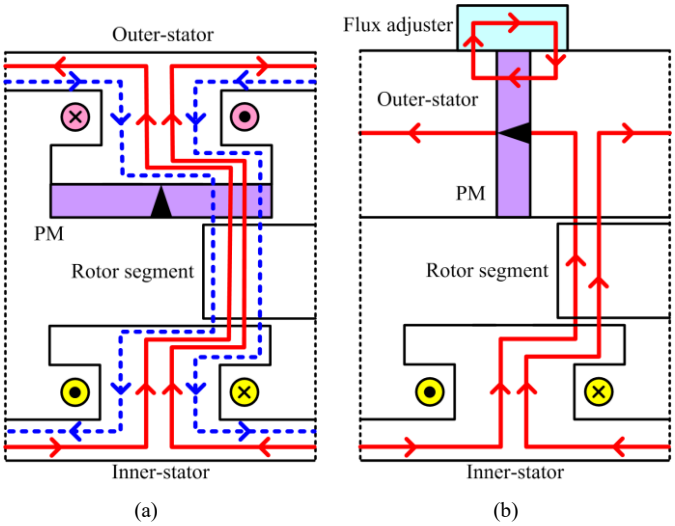

Fig. 5. Flux-weakening operations: (a) PS-FSHE. (b) FA-PS-FSPM.

TABLE I.
KEY MACHINE DESIGN PARAMETERS

Item	PS-FSDC	PS-FSHE	FA-PS-FSPM
Outer-stator outside diameter	269 mm	269 mm	269 mm
Outer-stator inside diameter	220 mm	220 mm	220 mm
Rotor outside diameter	219 mm	219 mm	219 mm
Rotor inside diameter	176 mm	176 mm	176 mm
Inner-stator outside diameter	175 mm	175 mm	175 mm
Inner-stator inside diameter	40 mm	40 mm	40 mm
Airgap length	0.5 mm	0.5 mm	0.5 mm
Stack length	84 mm	84 mm	84 mm
Number of stator slots	12	12	12
Number of rotor poles	10	10	10
Number of phases	3	3	3
Number of armature turns	33	33	33
Excitation source	DC	DC + PM	PM

C. Torque Performance Analysis

The output torque waveforms of the proposed machines at rated conditions are shown in Fig. 9. It can be observed that the average torques of the PS-FSDC machine under three situations, namely with DC-field excitations I_{DC} of 30 A/mm^2, 15 A/mm^2, and 5 A/mm^2 are around 218 Nm, 109 Nm, and 37 Nm, respectively. Meanwhile, the PS-FSHE machine under three situations, namely with I_{DC} of 30 A/mm^2, 0 A/mm^2 and −30 A/mm^2 are about 279 Nm, 163 Nm, and 41 Nm, respectively. On the other hand, the FA-PS-FSPM machine under two situations, namely with FAs, and without FAs installations are around 268 Nm, and 56 Nm, respectively.

Moreover, the torque ripple value T_{ripple} can be calculated based on the following relationship:

$$T_{ripple} = \frac{T_{\max} - T_{\min}}{T_{avg}} \; x \; 100\ \% \qquad (2)$$

where T_{avg}, T_{max}, and T_{min} are the average, maximum, and minimum torque values, respectively. It can be observed that the torque ripples of the PS-FSDC machine in the corresponding situations are about 24.3 %, 28.5 %, and 31.5 %, while of the PS-FSHE machine are about 9.8 %, 13.6 %, and 18.1 %. In the meantime, the torque ripples of the FA-PS-FSPM machine are 11.4 %, and 16.1 %.

To offer a more comprehensive analysis of the torque qualities, the cogging torques of the proposed machines are shown in Fig. 10. As shown, the cogging torques of the PS-FSDC machine in the corresponding situations are about 18.9 Nm, 8.4 Nm, and 2.6 Nm, where it is around 8.7 %, 7.7 %, and 7.0 % of its steady torques. For the PS-FSHE machine, its cogging torques are about 22.1 Nm, 11.4 Nm, and 2.7 Nm, as 7.9 %, 7.0 %, and 6.6 % of its steady torques. In the meantime, for the FA-PS-FSPM machine, its cogging torques are 17.1 Nm, and 2.9 Nm, as 6.5 %, and 5.2 % of its steady torques.

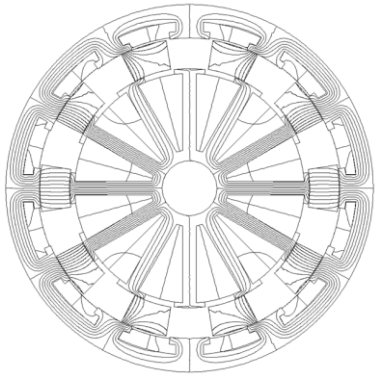

(a)

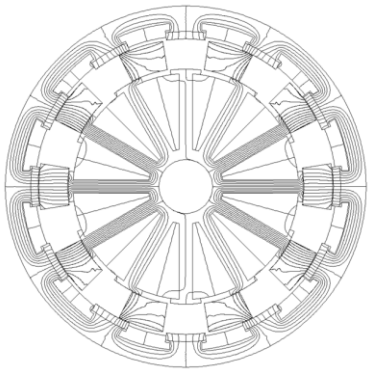

(b)

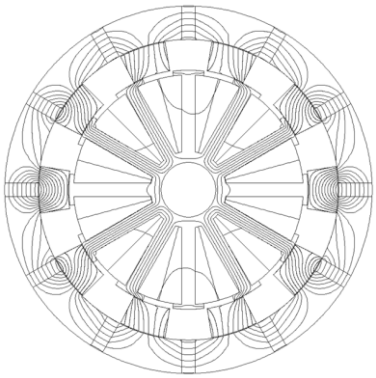

(c)

Fig. 6. Magnetic field distributions at no-load conditions: (a) PS-FSDC. (b) PS-FSHE. (c) FA-PS-FSPM.

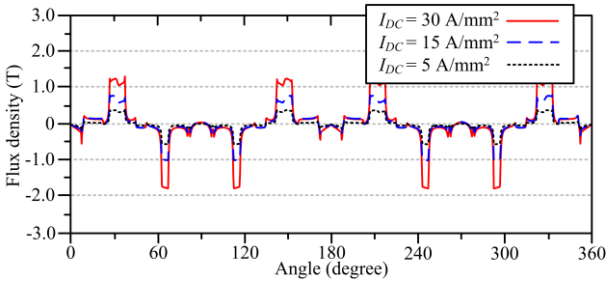

(a)

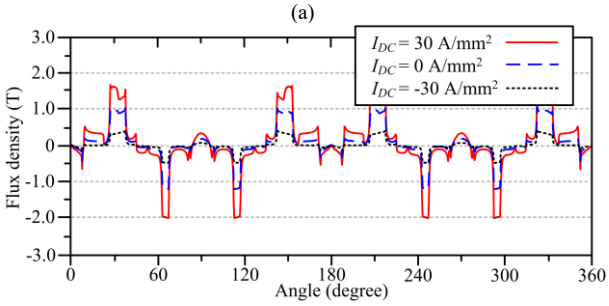

(b)

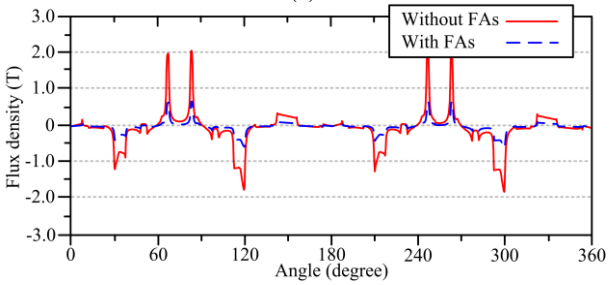

(c)

Fig. 7. Airgap flux densities: (a) PS-FSDC. (b) PS-FSHE. (c) FA-PS-FSPM.

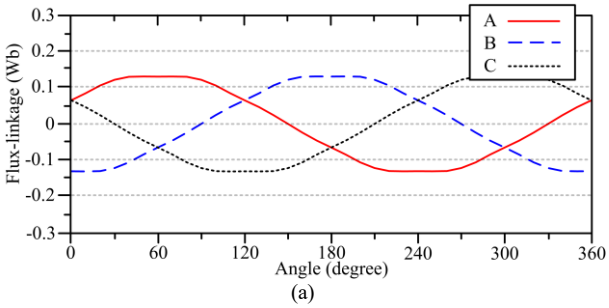

(a)

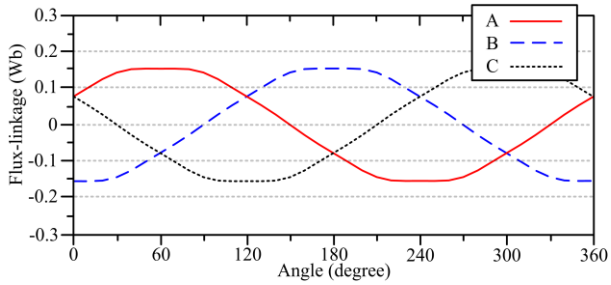

(b)

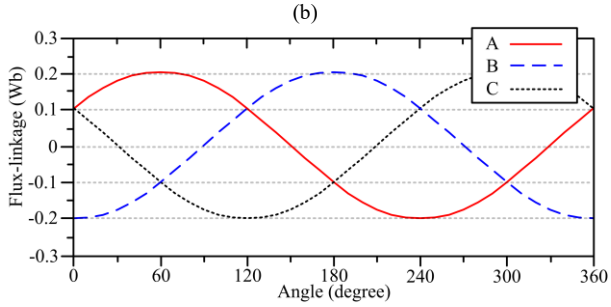

(c)

Fig. 8. Flux-linkages: (a) PS-FSDC. (b) PS-FSHE. (c) FA-PS-FSPM.

D. Flux-Weakening Analysis

The no-load EMF waveforms of the proposed machines with respect to different operating speeds are shown in Fig. 11. As expected, the no-load EMF values of all proposed machines increase along with the operating speeds.

With the help of the DC-field excitations, the PS-FSDC and PS-FSHE machines can both achieve satisfactory flux-weakening performances. It should be noted that the rated conditions, i.e., I_{DC} of 15 A/mm^2 for PS-FSDC machine and 0 A/mm^2 for PS-FSHE machine, are taken as the reference points for flux-weakening analysis. Since the PS-FSDC machine employs the DC-field current as the only excitation source, it can regulate its flux densities very effectively. In the meantime, with the DC-field current as the supplementary source, the PS-FSHE machine can only reduce its no-load EMFs for around 64 %, under the negative excitations of 30 A/mm^2.

On the other hand, unlike the other two machines that employ the DC-field windings for flux-regulations, the proposed FA-FSPM machine instead utilizes the mechanical FAs for flux-weakening operation. As shown, with the mechanical FAs installations, the reduction of no-load EMFs in the FA-PS-FSPM machine are about 76 %. It should be noted that the flux-weakening capability depends on the volume of the mechanical FAs. Therefore, the proposed FA-PS-FSPM machine can potentially achieve comparable flux-weakening capability to the PS-FSDC machine.

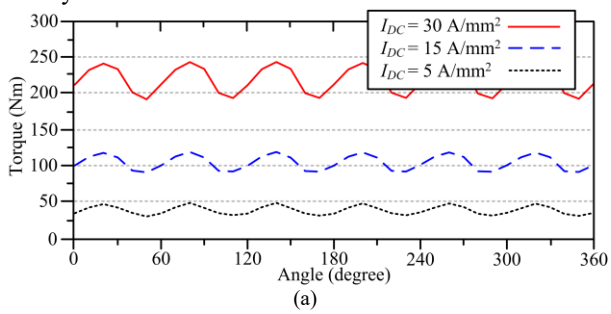

(a)

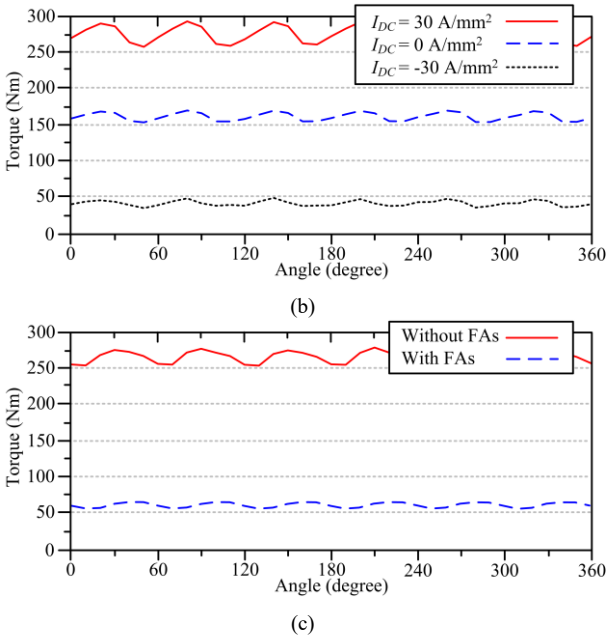

Fig. 9. Steady torques: (a) PS-FSDC. (b) PS-FSHE. (c) FA-PS-FSPM.

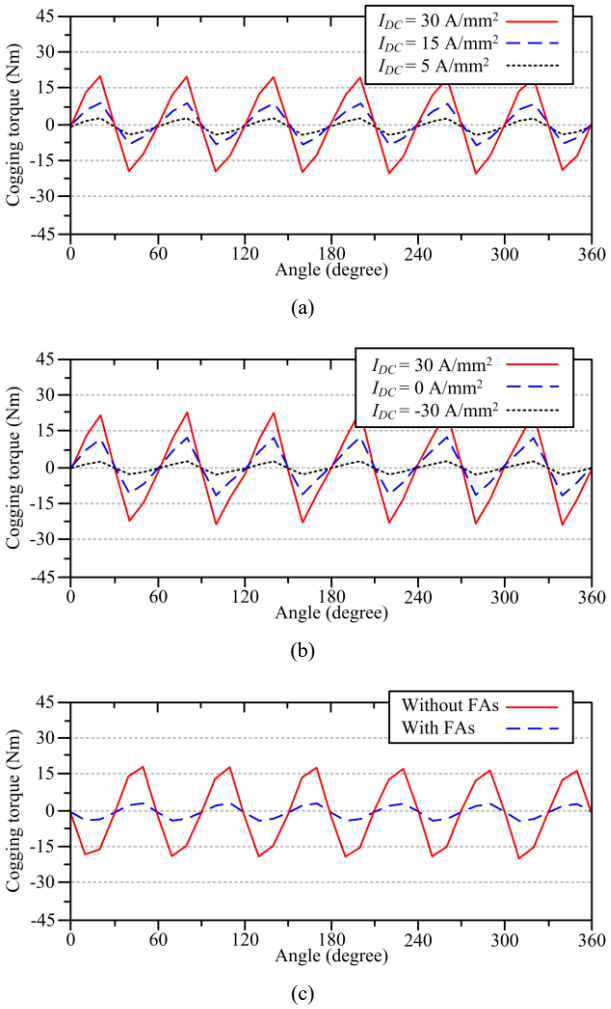

Fig. 10. Cogging torques: (a) PS-FSDC. (b) PS-FSHE. (c) FA-PS-FSPM.

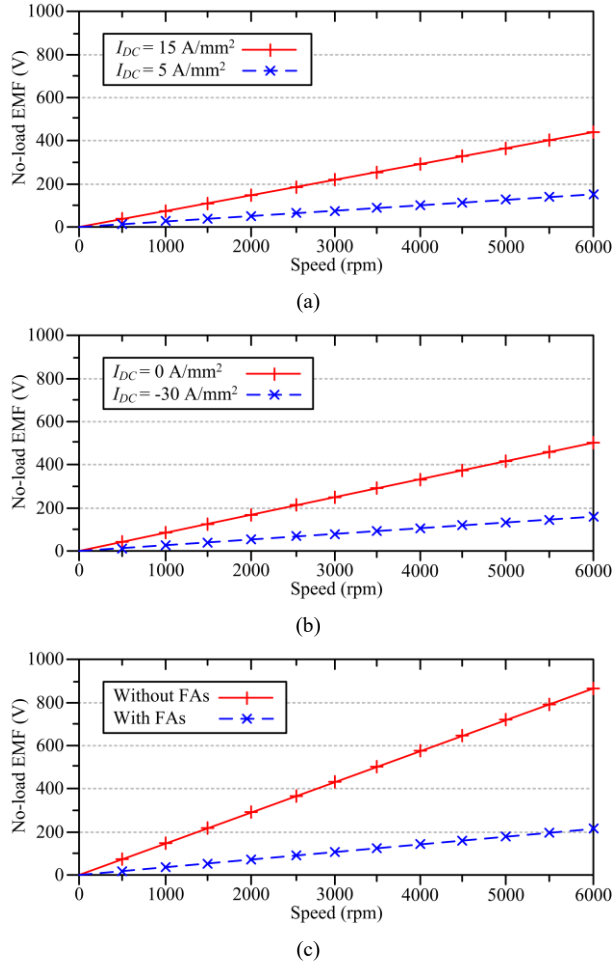

Fig. 11. No-load EMFs under flux-weakening operations: (a) PS-FSDC. (b) PS-FSHE. (c) FA-PS-FSPM.

TABLE II.
MACHINE PERFORMANCE COMPARISONS

Item	PS-FSPM	PS-FSHE	FA-PS-FSPM
Efficiency	81 %	83 %	88 %
Rated power	20500 W	30700 W	50000 W
Base speed	1800 rpm	1800 rpm	1800 rpm
Rated DC-field current	15 A/mm^2	0 A/mm^2	N/A
Rated torque	109 Nm	163 Nm	268 Nm
Torque ripple	28.5 %	13.6 %	11.4 %
Cogging torque	8.4 Nm	11.4 Nm	17.1 Nm
cogging torque %	7.7 %	7.0 %	6.5 %
Total mass	32.5 kg	28.9 kg	35.7 kg
Power density	630.8 W/kg	1062.3 W/kg	1400.2 W/kg
Torque density	3.4 Nm/kg	5.6 Nm/kg	7.4 Nm/kg
Material cost	44.6 US	107.1 US	122.4 US
Power / cost	459.6 W/US	286.6 W/US	408.5 W/US
Torque / cost	2.4 Nm/US	1.5 Nm/US	2.2 Nm/US

V. Evaluations on the Proposed Machines

For better illustration, all the major performances of the proposed machines are summarized in Table II. With the utilization of the high-energy-density PM materials as the major excitation sources, both the PS-FSHE and FA-PS-FSPM machines can achieve outstanding torque and power densities as compared with the PS-FSDC counterparts. To be specific, the proposed FA-PS-FSPM machine can achieve the highest torque and power densities among its competitors. As a result,

for the modern HEVs that require high torque densities for engine cranking, the PM candidates should be the best choice.

Aforementioned in the previous sessions, other than the engine cranking, the torque boosting is another important feature for the high-end HEV applications. Upon the support of the controllable DC-field excitation, the PS-FSDC and PS-FSHE machines can both generate satisfactory boosted torques for a short period of time. On the other hand, the FA-PS-FSPM machine can only increase the armature currents to achieve the same purpose.

Since the PS-FSDC and PS-FSHE machines have installed the independent DC-field excitations for flux-regulations, both of these two machines can provide desirable flux-weakening performances for wide-speed range operations. However, the DC-field currents produce the unfavorable copper losses that will reduce the overall efficiencies. In addition, the relatively high current densities require more sophisticated devices for heat dissipation management. Hence, the flux-regulating operations, especially the flux-strengthening operations, are only favorable for short duration of time. On the other hand, the FA-PS-FSPM machine utilizes the non-current-conductive approach, i.e., the mechanical FAs, for flux-weakening operation. Hence, the FA-PS-FSPM machine can enjoy more benefits, in terms on thermal management, from the flux-regulating operation.

Since all three proposed machines share the similar machine structures, i.e., all three of them employ the double-stator sandwiched-rotor structure, all three machines result with similar mechanical integrity and robustness. However, the FA-PS-FSPM machine requires additional mechanical devices, e.g., external servo machine, for the FA movement. Hence, when the whole machine system is overseen, the FA-PS-FSPM machine will suffer from relatively more complicated manufacturing processes and lower robustness.

Other than the vehicular performances, the cost-effectiveness has always been one of the key considerations for the potential HEV buyers [12]. To quantitatively compare this important factor, the key material costs, namely the laminated iron, PM material, and copper, have been extracted based on the market price. Consequently, both the FS-PSHE and FA-PS-FSPM machines can achieve very desirable cost-effectiveness for the potential stackers.

To offer a more user-friendly evaluations for the readers, a score grading system is adopted as shown in Table III. Six key criteria are categorized in the grading system and each of them is graded from score 1 to 5, where 1 indicates the worst and 5 the best. As a results, when all the important criteria are taken into considerations, the proposed FA-PS-FSPM machine will become the most promising candidate for HEV applications.

TABLE III
EVALUATIONS ON THE PROPOSED MACHINES

Item	PS-FSDC	PS-FSHE	FA-PS-FSPM
Efficiency	2	3	4
Power and torque densities	1	3	5
Flux-controllability	5	4	4
Mechanical Integrity	4	3	1
Thermal management	2	2	4
Cost-effectiveness	5	2	4
Total	19	17	22

VI. Conclusion

In this paper, three PS machines, namely the PS-FSDC, the PS-FSHE and the FA-PS-FSPM machines have been proposed and quantitatively compared. Based on the DC-field excitations, the PS-FSDC and PS-FSHE machines can both regulate their flux densities effectively. On the other hand, the FA-PS-FSPM machine instead employs the non-current-conductive FAs to short-circuit the PM fluxes. Hence, it can also produce satisfactory flux-weakening characteristic for wide-speed range operation. When all the key parameters are taken into considerations, the FA-PS-FSPM machine has been regarded as the most attractive candidate for the HEV applications.

References

[1] C. C. Chan, "The state of the art of electric, hybrid and fuel cell vehicles," *Proc. IEEE*, vol. 95, no. 4, pp. 704–718, Apr. 2007.

[2] Z. Q. Zhu, and D. Howe, "Electrical machines and drives for electric, hybrid, and fuel cell vehicles," *Proc. IEEE*, vol. 95, no. 4, pp. 746–765, Apr. 2007.

[3] A. Emadi, Y. J. Lee, and K. Rajashekara, "Power electronics and motor drives in electric, hybrid electric, and plug-in hybrid electric vehicles," *IEEE Trans. Ind. Electron*., vol. 55, no. 6, pp. 2237–2245, Jun. 2008.

[4] M. Cheng, W. Hua, J. Zhang, and W. Zhao, "Overview of stator-permanent magnet brushless machines," *IEEE Trans. Ind. Electron*., vol. 58, no. 11, pp. 5087–5101, Nov. 2011.

[5] A. Tenconi, S. Vaschetto, and A. Vigliani, "Electrical machines for high-speed applications: Design considerations and tradeoffs," *IEEE Trans. Ind. Electron*., vol. 61, no. 6, pp. 3022–3029, Jun. 2014.

[6] K. T. Chau, Electric Vehicle Machines and Drives–Design, Analysis and Application. New York, NY, USA: Wiley, 2015

[7] R. Cao, C. Mi, and M. Cheng, "Quantitative comparison of flux-switching permanent-magnet motors with Interior permanent magnet motor for EV, HEV, and PHEV applications," *IEEE Trans. Magn.*, vol. 48, no. 8, pp. 2374–2384, Dec. 2008.

[8] R. P Deodhar, A. Pride, S. Iwasaki, and J. J. Bremner, "Performance improvement in flux-switching PM machines using flux diverters," *IEEE Trans. Ind. Appl*., vol. 50, no. 2, pp. 937–978, Mar./Apr. 2014.

[9] W. Zhao, T. A. Lipo, and B. I. Kwon, "A novel dual-rotor, axial field, fault-tolerant flux-switching permanent magnet machine with high-torque performance," *IEEE Trans. Magn.*, vol. 51, no. 11, p. 8112204, Nov. 2015.

[10] D. J. Evans, and Z. Q. Zhu, "Novel partitioned stator switched flux permanent magnet machines," *IEEE Trans. Magn.*, vol. 51, no. 1, p. 8100114, Jan. 2015.

[11] I. Boldea, L. N. Tutelea, L. Parsa, and D. Dorrell, "Automotive electric propulsion systems with reduced or no permanent magnets: An overview," *IEEE Trans. Ind. Electron*., vol. 61, no. 10, pp. 5696–5711, Oct. 2014.

[12] C. H. T. Lee, K. T. Chau, and C. Liu, "Design and analysis of an electronic-geared magnetless machine for electric vehicles," *IEEE Trans. Ind. Electron*., vol. 63, no. 11, pp. 6705–6714, Nov. 2016.

[13] Z. Xu, S. Xie, and P. Mao, "Analytical design of flux-switching hybrid excitation machine by a nonlinear magnetic circuit method," *IEEE Trans. Magn.*, vol. 49, no. 6, pp. 3002–3008, Jun. 2013.

[14] B. Gaussens, E. Hoang, M. Lecrivain, P. Manfe, and M. Gabsi, "A hybrid-excited flux-switching machine for high-speed DC-alternator applications," *IEEE Trans. Ind. Electron*., vol. 61, no. 6, pp. 2976–2989, Jun. 2014.

[15] W. Hau, Xiaomei, Yin, G. Zhang, and M. Cheng, "Analysis of two novel five-phase hybrid-excitation flux-switching machines for electric vehicles," *IEEE Trans. Magn.*, vol. 50, no. 11, p. 8700305, Nov. 2014.

[16] Z. Q. Zhu, M. M. J. Al-Ani, X. Liu, and B. Lee, "A mechanical flux weakening method for switched flux permanent magnet machines," *IEEE Trans. Energy Convers.*, vol. 30, no. 2, pp. 806–815, Jun. 2015.

[17] C. H. T. Lee, J. L. Kirtley, and M. Angle, "A partitioned-stator flux-switching permanent-magnet machine with mechanical flux adjusters for hybrid electric vehicles," *IEEE Trans. Magn.*, to appear.

Christopher H. T. Lee (M'12) received the B.Eng. (first class honours) degree, and Ph.D. degree both in electrical engineering from Department of Electrical and Electronic Engineering, The University of Hong Kong, Hong Kong.

He currently serves as the Postdoctoral Fellow in Research Laboratory of Electronics, Massachusetts Institute of Technology. His research interests include electric motors and drives, renewable energies, and electric vehicle technologies. He is the author and co-author of 3 book chapters, 2 patents, and over 50 international referred papers.

Dr. Lee received the Croucher Foundation Fellowship 2016/2017 to support his postdoctoral research.

James L. Kirtley Jr. is a Professor of Electrical Engineering at the Massachusetts Institute of Technology (MIT). He was with General Electric, Large Steam Turbine Generator Department, as an Electrical Engineer, Satcon Technology Corporation as Vice President and General Manager of the Tech Center, as Chief Scientist and Director. Dr. Kirtley was Gastdozent at the Swiss Federal Institute of Technology, Zürich (ETH).

Dr. Kirtley attended MIT as an undergraduate and received the degree of Ph.D. from MIT in 1971. Dr. Kirtley is a specialist in electric machinery and electric power systems. He served as Editor in Chief of the IEEE Transactions on Energy Conversion from 1998 to 2006. Dr. Kirtley was made a Fellow of IEEE in 1990. He was awarded the IEEE Third Millennium medal in 2000 and the Nikola Tesla prize in 2002. Dr. Kirtley was elected to the United States National Academy of Engineering in 2007. He is a Registered Professional Engineer in Massachusetts.

Heng Nian (M'09，SM'14) received the B.Eng. degree and the M.Eng. degree from HeFei University of Technology, China, and the Ph.D. degree from Zhejiang University, China, in 1999, 2002, and 2005 respectively, all in electrical engineering.

From 2005 to 2007, he was as a Post-Doctoral with the College of Electrical Engineering, Zhejiang University, China. In 2007, he was promoted as an Associate professor. Since 2016, he has been a Full Professor at the College of Electrical Engineering, Zhejiang University, China. From 2013 to 2014, he was a visiting scholar at the Department of Electrical, Computer, and System Engineering, Rensselaer Polytechnic Institute, Troy, NY. His current research interests include the optimal design and operation control for wind power generation system. He has published more than 20 IEEE/IET Transaction papers and holds more than 20 issued/pending patents.